1996-09

Towards and FVE-FAC Method for Determining Thermocapillary Effects on Weld Pool Shape

Canright, David; Henson, Van Emden

TOWARDS AN FVE-FAC METHOD FOR DETERMINING THERMOCAPILLARY EFFECTS ON WELD POOL SHAPE

David Canright and Van Emden Henson
Mathematics Dept., Code MA
Naval Postgraduate School
Monterey, CA 93943

SUMMARY

Several practical materials processes, e.g., welding, float-zone purification, and Czochralski crystal growth, involve a pool of molten metal with a free surface, with strong temperature gradients along the surface. In some cases, the resulting thermocapillary flow is vigorous enough to convect heat toward the edges of the pool, increasing the driving force in a sort of positive feedback. In this work we examine this mechanism and its effect on the solid-liquid interface through a model problem: a half space of pure substance with concentrated axisymmetric surface heating, where surface tension is strong enough to keep the liquid free surface flat. The numerical method proposed for this problem utilizes a finite volume element (FVE) discretization in cylindrical coordinates. Because of the axisymmetric nature of the model problem, the control volumes used are torroidal prisms, formed by taking a polygonal cross-section in the (r, z) plane and sweeping it completely around the z-axis. Conservation of energy (in the solid), and conservation of energy, momentum, and mass (in the liquid) are enforced globally by integrating these quantities and enforcing conservation over each control volume. Judicious application of the Divergence Theorem and Stokes' Theorem, combined with a Crank-Nicolson time-stepping scheme leads to an implicit algebraic system to be solved at each time step.

It is known that near the boundary of the pool, that is, near the solid-liquid interface, the full conduction-convection solution will require extremely fine length scales to resolve the physical behavior of the system. Furthermore, this boundary moves as a function of time. Accordingly, we develop the foundation of an adaptive refinement scheme based on the principles of Fast Adaptive Composite Grid methods (FAC). Implementation of the method and numerical results will appear in a later report.

INTRODUCTION

Several practical materials processes, e.g., welding, float-zone purification, and Czochralski crystal growth, involve a pool of molten metal with a free surface, with

strong temperature gradients along the surface. In many cases (e.g., laser welding) convection in the liquid metal is driven primarily by thermocapillary forces, and even in cases where other forces are stronger overall, thermocapillary forces may still be dominant near the edge of the pool [4]. Previous work [2] showed how vigorous thermocapillary convection can lead to localized intense heat transfer and high velocities in the "cold corner" region where the liquid free surface meets the solid.

The present work examines how this localized heat transfer modifies the shape of the solid-liquid interface bounding the pool. When convection is vigorous, the high heat flux in the corner may melt away the solid near the surface, resulting in a sort of "lip" around the edge of the pool. This phenomenon is modeled computationally, and the steady solution sought for a wide range of the two governing parameters. This is a work in progress, in which numerical methods are proposed and developed for the problem. Implementation of the method and numerical results will appear in a later report.

PROBLEM STATEMENT

A half-space of a pure material is subjected to concentrated heating on the flat horizontal surface, giving a pool of molten material surrounded by solid. The total heat flux Q is constant, and far away the solid approaches the uniform cold temperature T_c (see Figure 1). Above the horizontal free surface is an inviscid, nonconducting gas. Surface tension of the liquid is assumed strong enough to keep the free surface flat (small Capillary number), but with surface tension variations due to a linear dependence on temperature. The resulting thermal and flow fields are assumed to be axisymmetric and steady, but the time-dependent equations are given below, to facilitate a numerical approach using time-like iterations to reach the steady solution.

Then the system is governed by conservation of energy in the solid and by conservation of energy, momentum, and mass in the pool:

$$\text{solid} \quad : \quad \frac{\partial T}{\partial t} = \kappa \nabla^2 T \tag{1}$$

$$\text{liquid} \quad : \quad \frac{\partial T}{\partial t} + \mathbf{u} \cdot \nabla T = \kappa \nabla^2 T \tag{2}$$

$$\frac{\partial \mathbf{u}}{\partial t} + \mathbf{u} \cdot \nabla \mathbf{u} = -\frac{1}{\rho} \nabla p + \nu \nabla^2 \mathbf{u} \tag{3}$$

$$\nabla \cdot \mathbf{u} = 0 \tag{4}$$

with the conditions at the boundaries and at the solid-liquid interface given by

$$\text{solid surface} \quad (z = 0) \quad : \quad \frac{\partial T}{\partial z} = 0 \tag{5}$$

$$\text{liquid surface} \quad (z = 0) \quad : \quad k \frac{\partial T}{\partial z} = -q(r) \tag{6}$$

$$v = 0 \tag{7}$$

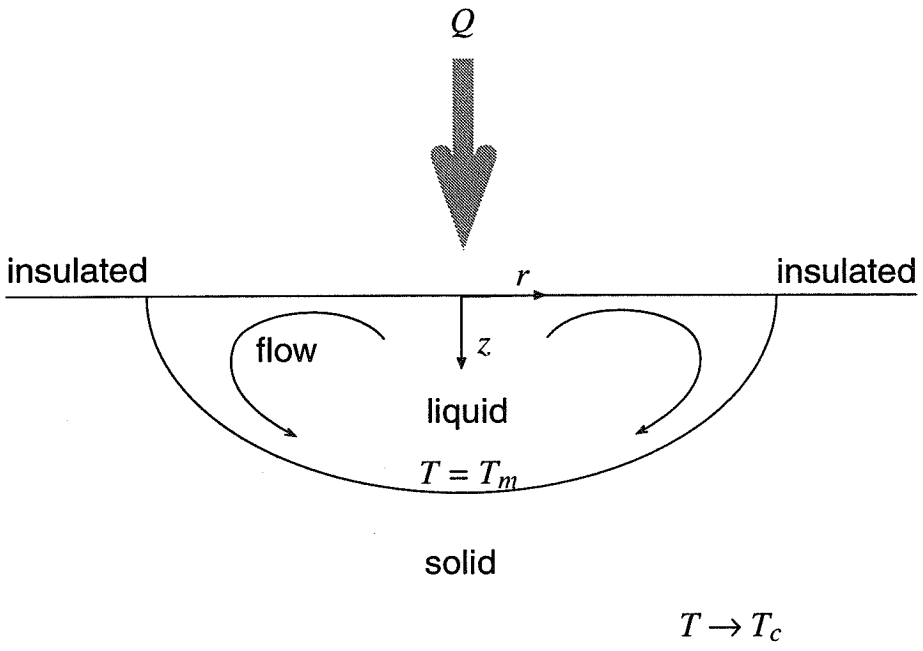

Figure 1: *Problem Formulation: a half-space of pure material is subjected to concentrated surface heating Q that results in a molten pool. (Outside the surface heating, the surface is adiabatic.) The melting temperature is T_m, and far away the solid is at the cooler temperature T_c. The flat liquid surface is subject to thermocapillary forcing, which drives convection in the liquid. Axisymmetry is assumed.*

$$\mu \frac{\partial u}{\partial z} = -\gamma \frac{\partial T}{\partial r} \tag{8}$$

$$\text{axis } (r = 0) \; : \quad \frac{\partial T}{\partial r} = 0 \tag{9}$$

$$u = 0 \tag{10}$$

$$\frac{\partial v}{\partial r} = 0 \tag{11}$$

$$\text{far away } (r, z \to \infty) \; : \quad T \to T_c \tag{12}$$

$$\text{interface } (r = f(z,t)) \; : \quad T = T_m \tag{13}$$

$$u = v = 0 \tag{14}$$

$$-(k \nabla T)_l = -(k \nabla T)_s + \rho L \mathbf{V}(z,t) \tag{15}$$

Here T is temperature, t is time, κ is thermal diffusivity, $\mathbf{u}$ is the velocity vector with components u and v in the r and z directions (cylindrical coordinates), ρ is density, p is pressure, ν is kinematic viscosity, k is thermal conductivity, $q(r)$ is the imposed surface heat flux (large at $r = 0$, falling off to zero at some small value of r, such that $\int_0^\infty q(r) 2\pi r \, dr = Q$), μ is viscosity, γ (assumed constant and positive) is the negative of the derivative of the surface tension with respect to temperature, T_m is the melting temperature, $r = f(z,t)$ gives the position of the solid-liquid interface, L is the latent heat of fusion, and $\mathbf{V}(z,t)$ is the normal velocity of the phase-change interface (that

is,

$$\mathbf{V}(z,t) = \frac{\partial f}{\partial t}/\sqrt{1+(\frac{\partial f}{\partial r})^2}\,\hat{\mathbf{n}}$$

where the unit normal vector is

$$\hat{\mathbf{n}} = (\hat{\mathbf{r}} + \frac{\partial f}{\partial r}\hat{\mathbf{z}})/\sqrt{1+(\frac{\partial f}{\partial r})^2}$$

in terms of the coordinate unit vectors).

To nondimensionalize the equations, we use a heat flux scale of Q and a temperature scale (relative to the cold temperature) of $\Delta T \equiv T_m - T_c$. Then thermal conduction gives the length scale $d \equiv Q/k\Delta T$ (so q scales as $Q/d^2 = (k\Delta T)^2/Q$), the thermocapillary coupling gives the velocity scale $u_s \equiv \gamma\,\Delta T/\mu$, and the convection time scale is $t_c \equiv d/u_s = \mu Q/k\gamma\Delta T^2$. The viscous pressure scale is $\mu u_s/d = k\gamma\Delta T^2/Q$. From the phase-change condition, the phase-change time scale is $t_p \equiv \rho L Q^2/(k\Delta T)^3$.

The resulting dimensionless equations are

$$\text{solid} \quad : \quad Ma\,\frac{\partial T}{\partial t} = \nabla^2 T \tag{16}$$

$$\text{liquid} \quad : \quad Ma\left(\frac{\partial T}{\partial t} + \mathbf{u}\cdot\nabla T\right) = \nabla^2 T \tag{17}$$

$$Re\left(\frac{\partial \mathbf{u}}{\partial t} + \mathbf{u}\cdot\nabla\,\mathbf{u}\right) = -\nabla p + \nabla^2\,\mathbf{u} \tag{18}$$

$$\nabla\cdot\mathbf{u} = 0 \tag{19}$$

with the boundary conditions

$$\text{solid surface} \ (z=0) \quad : \quad \frac{\partial T}{\partial z} = 0 \tag{20}$$

$$\text{liquid surface} \ (z=0) \quad : \quad \frac{\partial T}{\partial z} = -q(r) \tag{21}$$

$$v = 0 \tag{22}$$

$$\frac{\partial u}{\partial z} = \frac{\partial T}{\partial r} \tag{23}$$

$$\text{axis} \ (r=0) \quad : \quad \frac{\partial T}{\partial r} = 0 \tag{24}$$

$$u = 0 \tag{25}$$

$$\frac{\partial v}{\partial r} = 0 \tag{26}$$

$$\text{far away} \ (r, z \to \infty) \quad : \quad T \to 0 \tag{27}$$

$$\text{interface} \ (r = f(z,t)) \quad : \quad T = 1 \tag{28}$$

$$u = v = 0 \tag{29}$$

$$-\nabla T_l = -\nabla T_s + \lambda\mathbf{V} \tag{30}$$

where from this point on the variables denote the dimensionless quantities. The main dimensionless parameters are the Marangoni number $Ma \equiv u_s d/\kappa = \gamma Q/\mu k\kappa$ and

the Reynolds number $Re \equiv u_s d/\nu$. Their ratio gives the Prandtl number: $Pr \equiv \nu/\kappa = Ma/Re$. The other dimensionless parameter is the ratio of time scales, $\lambda \equiv t_p/t_c = \gamma QL/\nu k^2 \Delta T$, and so plays no role in the steady-state solution where $\mathbf{V} \to \mathbf{0}$.

For the numerical solutions, it is convenient to eliminate the pressure by adopting a stream-function/vorticity formulation for the flow:

$$Re\left(\frac{\partial \omega}{\partial t} - \nabla \times (\mathbf{u} \times \omega)\right) = -\nabla \times \nabla \times \omega \tag{31}$$

$$\omega = \nabla \times \nabla \times \left(\frac{\Psi}{r}\hat{\theta}\right) \tag{32}$$

$$u = -\frac{1}{r}\frac{\partial \Psi}{\partial z} \quad , \quad v = \frac{1}{r}\frac{\partial \Psi}{\partial r} \tag{33}$$

where Ψ is the axisymmetric stream function and ω is the vorticity vector (having only one component, in the $\hat{\theta}$ direction), with the flow boundary conditions

$$\text{liquid surface } (z = 0) \; : \; \Psi = 0 \tag{34}$$

$$\omega = \frac{\partial T}{\partial r} \tag{35}$$

$$\text{axis } (r = 0) \; : \; \Psi = 0 \tag{36}$$

$$\omega = \mathbf{0} \tag{37}$$

$$\text{interface } (r = f(z,t)) \; : \; \Psi = \frac{\partial \Psi}{\partial r} = \frac{\partial \Psi}{\partial z} = 0 \tag{38}$$

With the assumption of small Capillary number, the resulting small surface deflection can be determined as a small perturbation to the flat interface from the dimensionless normal stress condition at the surface:

$$-p + 2\frac{\partial v}{\partial z} = Ca^{-1}\frac{1}{r}\frac{d}{dr}\left(r\frac{dh}{dr}\right) \tag{39}$$

where $Ca \equiv \gamma \Delta T/\sigma$ is the Capillary number for surface tension σ, and the deflection $z = h(r)$ is taken positive upward. The contact line at the edge of the pool is assumed pinned ($h = 0$), and volume is conserved globally to determine the constant reference pressure level.

CONDUCTION SOLUTIONS

As a starting point for the numerical method, an analytic solution for the temperature in the conductive limit is used; this limit corresponds to $Ma \to 0$ (for which the time scale used in nondimensionalizing is inappropriate). If the unit surface heat input were concentrated at a single point, then the conductive solution would have spherical symmetry:

$$T(r,z) = \frac{1}{2\pi R} \quad , \quad R \equiv \sqrt{r^2 + z^2} \tag{40}$$

For a distributed (axisymmetric) heat source $q(r)$, the point source solution (40) can be used as a Green's function, and the solution found by superposition:

$$T(r,z) = \int_0^\infty \int_0^{2\pi} \frac{q(\rho)\,\rho\,d\theta\,d\rho}{2\pi\sqrt{\rho^2+r^2-2\rho r\cos\theta+z^2}} \tag{41}$$

$$= \int_0^\infty \frac{q(\rho)\,\rho}{\sqrt{(\rho+r)^2+z^2}}\,{}_2F_1(\tfrac{1}{2},\tfrac{1}{2};1;\frac{4\rho r}{(\rho+r)^2+z^2})\,d\rho \tag{42}$$

where ${}_2F_1$ is the generalized hypergeometric function (see [1]). This formula can be used to find the temperature for any input heating distribution q, and the isotherm $T=1$ specifies the interface position.

Using this thermal solution with the interface position fixed, the flow equations (31)–(38) are solved numerically in the viscous limit $Re \to 0$ (again, the time scale used is inappropriate in this limit). This gives the basic state, which has no fine details (except near the concentrated heating, where the flow can be described by an asymptotic solution [3]). This state is used as a starting point for solutions with low Ma and high Pr.

NUMERICAL METHODS

For computational purposes, the idealized problem of an unbounded solid is truncated to a finite domain in cylindrical coordinates, extending in both the radial and vertical directions a distance of four times the diffusion length scale d. The boundary condition on this artificial boundary is that the temperature should decay in the same way as the conduction solution for the point source, that is,

$$\frac{\partial T}{\partial R} = -\frac{T}{R} \tag{43}$$

where $R=\sqrt{r^2+z^2}$ is the spherical coordinate. This asymptotic matching condition is reasonable (for several diffusion lengths away from the pool) and is far less restrictive than imposing the Dirichlet condition ($T=0$) on the outer boundary.

To calculate the steady state for various values of Ma and Pr, the time-dependent equations are stepped in time using the Crank-Nicholson method to obtain the advantages of absolute stability and large time steps. Then at each time step, an elliptic problem must be solved. For this, multilevel methods are used, based on a uniform grid in the (r,z) quarter-plane and the Fast Adaptive Composite (FAC) grid approach to ensure resolution of all small-scale local details. At the solid-liquid interface, each grid has irregular elements to fit the interface. At each time step, the position of the interface is adjusted based on the normal velocity V from (30). (Note that the dimensionless parameter λ in (30) can be adjusted to control how quickly the interface changes.) The difference equations on the grid are developed using the Finite Volume Element (FVE) method. This method combines the exact conservation of mass, momentum, and energy of the finite volume method with the flexibility of the

finite element method in handling complicated boundary conditions, irregular grids, etc. (See [5] for an introduction to FAC and FVE methods.) The resulting system of algebraic equations is solved at each time step. FAC is a method in which the solutions at the various grid levels are used to correct the composite grid solution, and the type of solver used on each grid level is unimportant. In this work both direct methods and iterative solution by line relaxation are used as solvers at each grid level.

FVE STENCILS

To recapitulate, the complete system of dimensionless equations is

$$\text{solid:} \qquad \frac{\partial T}{\partial t} = \frac{1}{Ma}\nabla\cdot\nabla T \tag{44}$$

$$\text{liquid:} \qquad \frac{\partial T}{\partial t} + \nabla\cdot(\mathbf{u}T) = \frac{1}{Ma}\nabla\cdot\nabla T \tag{45}$$

$$\frac{\partial \omega}{\partial t} - \nabla\times(\mathbf{u}\times\omega) = -\frac{1}{Re}\nabla\times\nabla\times\omega \tag{46}$$

$$\omega = \nabla\times\nabla\times\left(\frac{\Psi}{r}\hat{\theta}\right) \tag{47}$$

$$\text{where} \qquad \mathbf{u} = \nabla\times\left(\frac{\Psi}{r}\hat{\theta}\right) = -\frac{1}{r}\frac{\partial\Psi}{\partial z}\hat{\mathbf{r}} + \frac{1}{r}\frac{\partial\Psi}{\partial r}\hat{\mathbf{z}} \tag{48}$$

with the boundary conditions

$$\text{solid surface } z=0 \;:\; \frac{\partial T}{\partial z} = 0 \tag{49}$$

$$\text{liquid surface } z=0 \;:\; \frac{\partial T}{\partial z} = -q(r) \tag{50}$$

$$\Psi = 0 \tag{51}$$

$$\omega = \frac{\partial T}{\partial r}\hat{\theta} \tag{52}$$

$$\text{axis } r=0 \;:\; \frac{\partial T}{\partial r} = 0 \tag{53}$$

$$\Psi = 0 \tag{54}$$

$$\omega = \mathbf{0} \tag{55}$$

$$\text{far away } r,z\to\infty \;:\; \frac{\partial T}{\partial R} \to -\frac{T}{R} \quad \left(\text{where } R\equiv\sqrt{r^2+z^2}\right) \tag{56}$$

$$\text{interface } r=f(z,t) \;:\; T = 1 \tag{57}$$

$$\Psi = \frac{\partial\Psi}{\partial n} = 0 \tag{58}$$

$$V_n = \lambda^{-1}\left[\left(\frac{\partial T}{\partial n}\right)_s - \left(\frac{\partial T}{\partial n}\right)_l\right] \tag{59}$$

where n refers to the direction normal to the interface (outward). (Note: $\int_0^\infty q(r)\,r\,dr = 1$.)

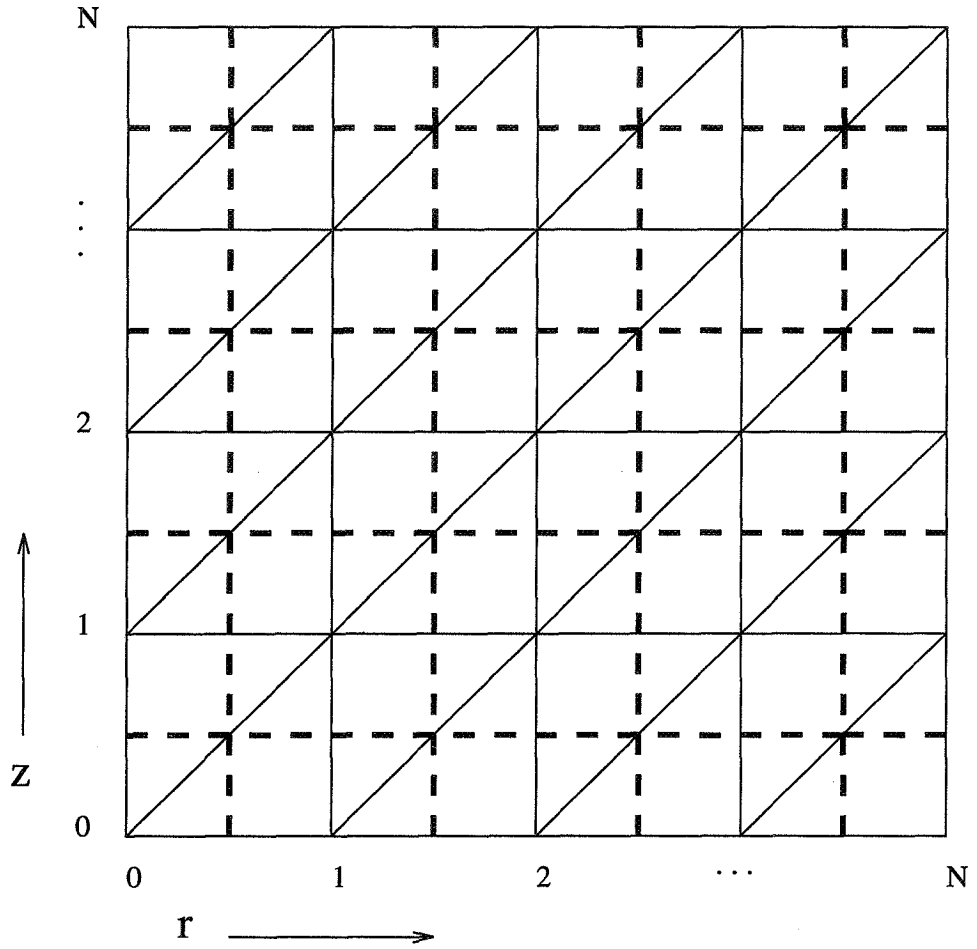

Figure 2: *FVE Grid: the orientation of the triangular finite elements (solid) and the square finite volumes (dashed) are shown. On each triangular element, the variables are assumed linear between the three nodes. This allows consistent calculation of the gradients across the volume boundaries. Note that this is only a cross section in the* (r, z) *plane; the volumes extend in the* θ *direction to form rings.*

The Finite Volume Element (FVE) approach to discretizing the system involves decomposing the domain in two ways: as the union of a set of elements, whose vertices compose the set of grid points on which the unknowns are defined; and as the union of a set of control volumes, one for each grid point (see Figure 2). The unknowns are interpolated over each element, based on the values at the grid points, giving a continuous representation over the whole domain. This representation is used to integrate the conservation equations over each control volume. Hence, each control volume gives three equations involving the three unknowns at the associated grid point, as well as the values at neighboring points. The resulting set of discrete equations for the finite element representation of the solution satisfies the conservation laws exactly over any volume made up of the union of control volumes, including the whole domain. (Actually, the boundary conditions may eliminate some of the control volumes.)

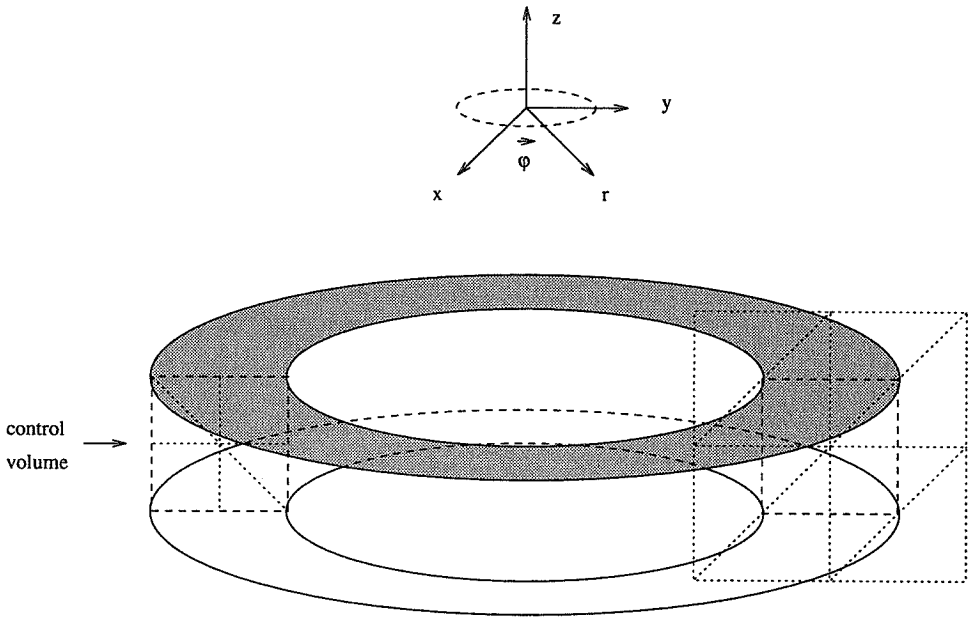

Figure 3: *From axisymmetry, each control volume results from sweeping the square cross-section in the (r, z) plane about the z axis, giving a toroidal prism shape. Hence, the uniform grid gives control volumes that increase with radial position.*

For this axisymmetric problem, each control volume is a toroidal prism, the result of taking a polygonal cross-section in the (r, z) plane and sweeping it all the way around in the θ direction (see Figure 3). Then, integrating the convection-diffusion equation (45) over a control volume, interchanging time derivatives and spatial integrals, and applying the divergence theorem gives

$$\frac{d}{dt} \iint_A T\, r\, dr\, dz + \oint_C \hat{\mathbf{n}} \cdot (\mathbf{u}T)\, r\, dl = \frac{1}{Ma} \oint_C \hat{\mathbf{n}} \cdot \nabla T\, r\, dl \tag{60}$$

where the 2π resulting from integration in θ has been factored out, A refers to the cross-sectional area (polygon) of the volume, C refers to the closed curve bounding that cross-section, and $\hat{\mathbf{n}}$ is the unit vector normal (outward) to C.

For the vorticity (46) and stream function equations (47), the control volume is a vorticity tube, and the appropriate integral is over the cross-sectional area A (with normal vector $\hat{\theta}$). Then, applying Stokes' theorem gives

$$\frac{d}{dt} \iint_A \omega \cdot \hat{\theta}\, dr\, dz - \oint_C \hat{\mathbf{t}} \cdot (\mathbf{u} \times \omega)\, dl = -\frac{1}{Re} \oint_C \hat{\mathbf{t}} \cdot \nabla \times \omega\, dl \tag{61}$$

$$\oint_C \hat{\mathbf{t}} \cdot \mathbf{u}\, dl = \iint_A \omega \cdot \hat{\theta}\, dr\, dz \tag{62}$$

where $\hat{\mathbf{t}}$ is the unit vector tangent to C, in the positive θ sense.

Except near the phase-change interface, a uniform grid is applied with step size h in both the r and z directions (see Figure 2). (Portions of this grid may be subdivided into smaller uniform grids by the FAC method.) Each square of the grid is divided

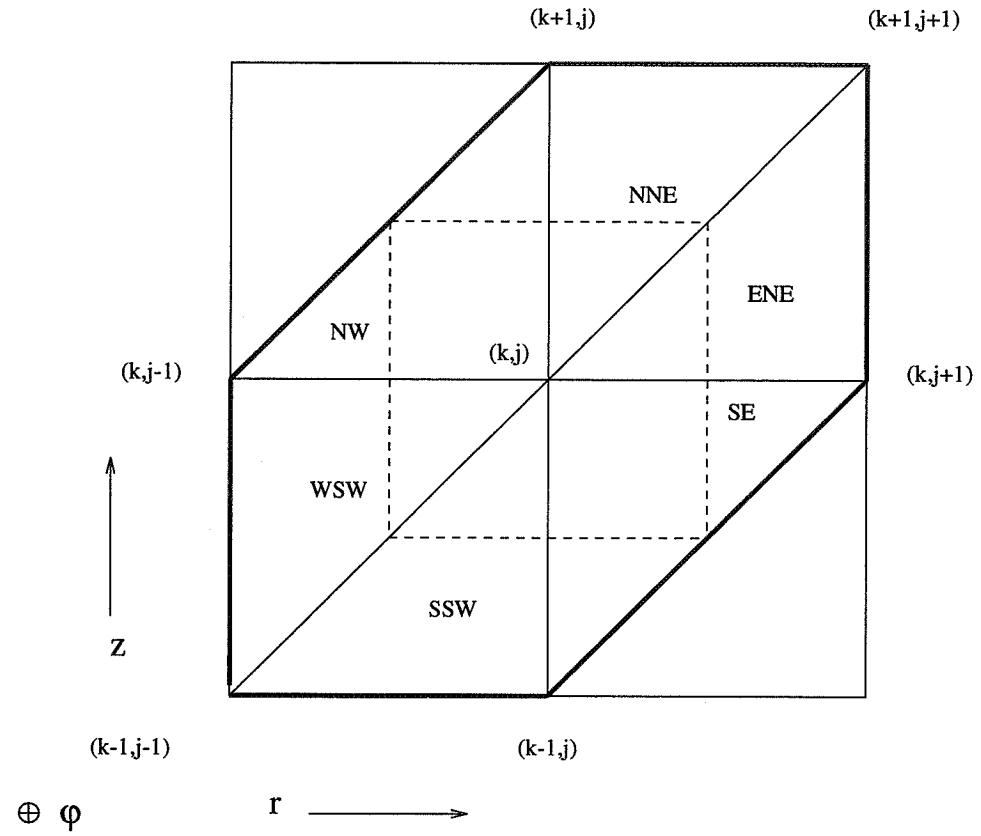

Figure 4: *The conservation integrals for each control volume cross-section involve six separate area integrals over the six triangular elements adjoining the central point; the line integrals involve eight separate parts (the NW and SE elements each contain two segments).*

into two triangular elements by a diagonal (in the direction of increasing $r + z$), and linear interpolation is used over each triangular element. The control volume cross sections are squares of side h, centered on each grid point (except for half-squares at the boundaries and small quarter-squares at the corners).

Then in the integrated conservation equations (60, 61, 62), the area integrals are over six triangular regions (portions of the six elements), and the line integrals are over four line segments, each with halves in two different elements (see Figure 4). In terms of components, the integrated equations are

$$\begin{aligned} \frac{d}{dt}\iint_A T\, r\, dr\, dz \;+\; & \int_N \frac{\partial \Psi}{\partial r} T\, dr - \int_E \frac{\partial \Psi}{\partial z} T\, dz - \int_S \frac{\partial \Psi}{\partial r} T\, dr + \int_W \frac{\partial \Psi}{\partial z} T\, dz \\ = \; & \frac{1}{Ma}\left(\int_N \frac{\partial T}{\partial z} r\, dr + \int_E \frac{\partial T}{\partial r} r\, dz - \int_S \frac{\partial T}{\partial z} r\, dr - \int_W \frac{\partial T}{\partial r} r\, dz \right), \end{aligned} \tag{63}$$

$$\frac{d}{dt}\iint_A \omega\, dr\, dz \;+\; \int_N \frac{\partial \Psi}{\partial r}\frac{\omega}{r} dr - \int_E \frac{\partial \Psi}{\partial z}\frac{\omega}{r} dz - \int_S \frac{\partial \Psi}{\partial r}\frac{\omega}{r} dr + \int_W \frac{\partial \Psi}{\partial z}\frac{\omega}{r} dz$$

$$= \frac{1}{Re}\left(\int_N \frac{\partial \omega}{\partial z}\,dr + \int_E \frac{\partial (r\,\omega)}{\partial r}\frac{1}{r}\,dz - \int_S \frac{\partial \omega}{\partial z}\,dr - \int_W \frac{\partial (r\,\omega)}{\partial r}\frac{1}{r}\,dz\right), \tag{64}$$

$$-\iint_A \omega\,dr\,dz = \int_N \frac{\partial \Psi}{\partial z}\frac{1}{r}\,dr + \int_E \frac{\partial \Psi}{\partial r}\frac{1}{r}\,dz - \int_S \frac{\partial \Psi}{\partial z}\frac{1}{r}\,dr - \int_W \frac{\partial \Psi}{\partial r}\frac{1}{r}\,dz, \tag{65}$$

where from here onward, ω refers to the one nonzero component of vorticity, and the labels N, E, S, and W refer to the four line segments of the line integrals by "compass direction" relative to the central node.

Substituting the piecewise linear element representation of the unknowns into the above integrals gives the discrete (in space) equations. (We use *Maple* to evaluate and sum the integrals for these equations.) The equations are then presented in stencil notation. In stencil notation, for example

$$\begin{pmatrix} a & b & c \\ d & e & f \\ g & h & i \end{pmatrix} T,$$

where the center of the matrix e is the coefficient of T at the gridpoint P, the other entries (a, $b\ldots$) in the matrix are the coefficients of the values the unknown (T) at the neighboring gridpoints, and r and z are horizontal and vertical coordinates of P, respectively. Blank entries indicate zero coefficients, and a central Σ indicates the sum of all the other coefficients in the matrix. Note that in the nonlinear convective terms, each of the coefficients of T or ω is itself expressed as a stencil in Ψ (each centered at the same point P); to save space, the Ψ is left out of the vorticity convection stencil.

At a typical grid point, the discretized equations become

$$\frac{d}{dt}\frac{h^2}{24}\begin{pmatrix} & 2-\frac{5}{16}\epsilon & 1+\frac{5}{16}\epsilon \\ 2-\frac{11}{16}\epsilon & 14 & 2+\frac{11}{16}\epsilon \\ 1-\frac{5}{16}\epsilon & 2+\frac{5}{16}\epsilon & \end{pmatrix} T$$

$$+\frac{1}{8r}\begin{pmatrix} & & \begin{pmatrix} & & 1 \\ -2 & 1 & \end{pmatrix}\Psi & \begin{pmatrix} & -1 & \\ & & 1 \end{pmatrix}\Psi \\ \begin{pmatrix} & 2 & \\ & -1 & \\ -1 & & \end{pmatrix}\Psi & \begin{pmatrix} & -1 & \\ 1 & & 1 \\ & -1 & \end{pmatrix}\Psi & \begin{pmatrix} & & -1 \\ & -1 & \\ 2 & & \end{pmatrix}\Psi \\ \begin{pmatrix} 1 & & \\ & -1 & \end{pmatrix}\Psi & \begin{pmatrix} & 1 & -2 \\ 1 & & \end{pmatrix}\Psi & \end{pmatrix} T$$

$$= \frac{1}{Ma}\begin{pmatrix} & 1 & \\ 1-\frac{1}{2}\epsilon & -4 & 1+\frac{1}{2}\epsilon \\ & 1 & \end{pmatrix} T \tag{66}$$

$$\frac{d}{dt}\frac{h^2}{24}\begin{pmatrix} & 2 & 1 \\ 2 & 14 & 2 \\ 1 & 2 & \end{pmatrix}\omega + \frac{1}{8r}\begin{pmatrix} & [A_1]\Psi & [A_2]\Psi \\ [A_3]\Psi & [C_A]\Psi & [A_4]\Psi \\ [A_5]\Psi & [A_6]\Psi & \end{pmatrix}\omega$$
$$= \frac{1}{Re}\begin{pmatrix} & 1-\frac{1}{8}\epsilon^+ & \frac{1}{8}\epsilon^- \\ 1-\frac{3}{8}\epsilon^+ & -\left[4+\frac{3}{8}(\epsilon^+-\epsilon^-)\right] & 1+\frac{3}{8}\epsilon^- \\ -\frac{1}{8}\epsilon^+ & 1+\frac{1}{8}\epsilon^- & \end{pmatrix}\omega \tag{67}$$

$$\begin{pmatrix} & 1 & \\ 1^+ & -[2+1^+ +1^-] & 1^- \\ & 1 & \end{pmatrix}\Psi = -\frac{rh^2}{24}\begin{pmatrix} & 2 & 1 \\ 2 & 14 & 2 \\ 1 & 2 & \end{pmatrix}\omega \tag{68}$$

where the internal stencils

$$[C_A]\Psi \equiv \begin{pmatrix} & -1+\frac{1}{2}\epsilon^+ & \epsilon^- \\ 1+\epsilon^+ & -\epsilon^+ +\epsilon^- & 1-\epsilon^- \\ -\epsilon^+ & -1-\frac{1}{2}\epsilon^- & \end{pmatrix}\Psi,$$

$$[A_1] \equiv \begin{pmatrix} & \frac{1}{2}\epsilon^+ & 1 \\ -2 & 1-\frac{1}{2}\epsilon^+ & \end{pmatrix}, \qquad [A_2] \equiv \begin{pmatrix} & -1 & \frac{1}{2}\epsilon^- \\ & & 1^- \\ & & \end{pmatrix},$$

$$[A_3] \equiv \begin{pmatrix} & 2+1^+ & \\ \frac{1}{2}\epsilon^+ & -1-\epsilon^+ & \\ -1^+ & & \end{pmatrix}, \qquad [A_4] \equiv \begin{pmatrix} & & -1^- \\ & -1+\epsilon^- & -\frac{1}{2}\epsilon^- \\ & 2+1^- & \end{pmatrix},$$

$$[A_5] \equiv \begin{pmatrix} & 1^+ & \\ -\frac{1}{2}\epsilon^+ & -1 & \end{pmatrix}, \qquad [A_6] \equiv \begin{pmatrix} & 1+\frac{1}{2}\epsilon^- & -2 \\ 1 & -\frac{1}{2}\epsilon^- & \end{pmatrix},$$

and the definitions

$$\epsilon \equiv h/r, \quad \epsilon^+ \equiv \frac{\epsilon}{1-\epsilon/2}, \quad \epsilon^- \equiv \frac{\epsilon}{1+\epsilon/2}, \quad 1^+ \equiv \frac{1}{1-\epsilon/2}, \quad 1^- \equiv \frac{1}{1+\epsilon/2},$$

are employed and r is the radial coordinate at the central point P. Note that for those integrals in r with integrands containing $1/r$, that factor was pulled outside the integral to avoid logarithms; the error introduced is of the same order as that due to the piecewise linear representation itself. Also, the heat equation was rescaled by $1/r$, and the stream function equation was rescaled by r.

The radial dependence of the coefficients is a direct result of the axisymmetric geometry. This dependence makes the calculation somewhat more complicated than the corresponding two-dimensional problem. But far from the axis, where $r \gg h$ and hence $\epsilon \ll 1$, the equations approach the corresponding two-dimensional versions, facilitating comparison.

Discretized Boundary Conditions

Along the surface $z = 0$, each of the three boundary conditions for the three unknowns requires different treatment. The temperature at each grid point along the surface is determined by a heat balance over the corresponding control volume, with a half-square cross section $(h \times h/2)$. The contribution of the surface to the convective flux integral is zero, since there is no velocity normal to the surface, and the contribution of the surface to the diffusive flux integral is given by the Neumann type boundary condition $\int q(r) r\, dr$. The resulting discrete equation is

$$\frac{d}{dt}\frac{h^2}{24}\begin{pmatrix} & 2-\frac{5}{16}\epsilon & 1+\frac{5}{16}\epsilon \\ \frac{3}{2}-\frac{1}{2}\epsilon & 7+\frac{5}{16}\epsilon & \frac{1}{2}+\frac{3}{16}\epsilon \end{pmatrix} T$$

$$+\ \frac{1}{8r}\begin{pmatrix} & & \begin{pmatrix} & 1 \\ & \end{pmatrix}\Psi & \begin{pmatrix} & -1 \\ & \end{pmatrix}\Psi \\ \begin{pmatrix} & 2 \\ & \end{pmatrix}\Psi & \begin{pmatrix} & -1 \\ & \end{pmatrix}\Psi & \begin{pmatrix} & -1 \\ & \end{pmatrix}\Psi \end{pmatrix} T$$

$$=\ \frac{1}{Ma}\begin{pmatrix} & 1 & \\ \frac{1}{2}-\frac{1}{4}\epsilon & -2 & \frac{1}{2}+\frac{1}{4}\epsilon \end{pmatrix} T + \frac{1}{r\,Ma}\int_{r-h/2}^{r+h/2} q(r) r\, dr \qquad (69)$$

Here we specify the heat flux as a symmetric function of r that decays smoothly to zero at some finite radius ρ_{max}, while satisfying $\int_0^\infty q(r) r\, dr = 1$:

$$q(r) \equiv \begin{cases} \frac{6}{\rho_{max}^2}\left[1-\left(\frac{r}{\rho_{max}}\right)^2\right]^2, & r \le \rho_{max} \\ 0, & r > \rho_{max} \end{cases} \qquad (70)$$

For the calculations, we use $\rho_{max} = \frac{1}{4}$.

The thermocapillary stress condition at the surface specifies the vorticity: $\omega = \frac{\partial T}{\partial r}$. However, because of the linear interpolation between grid points, $\frac{\partial T}{\partial r}$ is not well defined at grid points on the surface. Hence, for the surface only, the vorticity is specified at half-grid points (i.e., $r = (i + \frac{1}{2})h$), and triangular finite elements are formed with neighboring points. This keeps the discretization of this important condition at the same order of accuracy as the other equations, but entails special treatment of the grid points next to the surface. The surface is also a streamline, where $\Psi = 0$ (Dirichlet condition). Using that fact and these special surface vorticity elements gives the following flow equations for points by the surface (a distance h from the surface):

$$\frac{d}{dt}\frac{h^2}{24}\begin{pmatrix} \frac{19}{8} & 2 & 1 \\ & 14\frac{1}{4} & \frac{11}{8} \end{pmatrix}\omega + \frac{d}{dt}\frac{h}{16}\begin{pmatrix} & \\ -1 & 1 \end{pmatrix} T + \frac{1}{8r}\begin{pmatrix} & [B_1]\Psi & [B_2]\Psi \\ [B_3]\Psi & [C_B]\Psi & [B_4]\Psi \end{pmatrix}$$

$$+\frac{1}{8rh}\begin{pmatrix} & & \\ [D_1] & [D_2] & [D_3] \end{pmatrix} T = \frac{1}{Re}\begin{pmatrix} & 1-\frac{1}{8}\epsilon^+ & \frac{1}{8}\epsilon^- \\ \frac{7}{8}-\frac{7}{16}\epsilon^+ & -\left[\frac{15}{4}+\frac{5}{16}\epsilon^+-\frac{7}{16}\epsilon^-\right] & \frac{7}{8}+\frac{5}{16}\epsilon^- \end{pmatrix}\omega$$

$$+\frac{1}{Re}\frac{1}{h}\begin{pmatrix} & & \\ -\frac{1}{2}+\frac{1}{8}\epsilon^+ & -\frac{1}{8}\epsilon^+-\frac{1}{8}\epsilon^- & \frac{1}{2}+\frac{1}{8}\epsilon^- \end{pmatrix} T \quad (71)$$

$$\begin{pmatrix} & 1 & \\ 1^+ & -[2+1^+ +1^-] & 1^- \end{pmatrix}\Psi = \frac{rh^2}{24}\begin{pmatrix} & 2 & 1 \\ \frac{19}{8} & 14\frac{1}{4} & \frac{11}{8} \end{pmatrix}\omega + \frac{rh}{16}\begin{pmatrix} & \\ -1 & 1 \end{pmatrix} T \quad (72)$$

where

$$[C_B] \equiv \begin{pmatrix} & -1+\frac{1}{2}\epsilon^+ & \epsilon^- \\ \frac{1}{2}+\frac{3}{4}\epsilon^+ & 1-\frac{1}{2}\epsilon^+ +\frac{3}{4}\epsilon^- & \frac{1}{4}-\epsilon^- \end{pmatrix}$$

$$[B_1] \equiv \begin{pmatrix} & \frac{1}{2}+\frac{3}{4}\epsilon^+\epsilon^+ & 1 \\ -2 & 1-\frac{1}{2}\epsilon^+ & \end{pmatrix}, \quad [B_2] \equiv \begin{pmatrix} -1 & \frac{1}{2}\epsilon^- \\ & 1^- \end{pmatrix},$$

$$[B_3] \equiv \begin{pmatrix} & 2+1^+ \\ \frac{1}{2}+\frac{3}{4}\epsilon^+ & -1-\epsilon^+ \end{pmatrix}, \quad [B_4]\begin{pmatrix} & -1^- \\ -\frac{5}{4}+\frac{3}{4}\epsilon^- & \frac{3}{4}-\frac{1}{2}\epsilon^- \end{pmatrix},$$

$$[D_1] \equiv \begin{pmatrix} -1^+ & -\frac{1}{4} & \frac{1}{4} \end{pmatrix}, \quad [D_2] \equiv \begin{pmatrix} 1^+ & -\frac{1}{2}-\frac{1}{2}\epsilon^+ & \frac{3}{2} \end{pmatrix},$$

$$\text{and} \quad [D_3] \equiv \begin{pmatrix} \frac{3}{4}+\frac{1}{2}\epsilon^+ & -\frac{7}{4} \end{pmatrix}$$

Along the z axis, symmetry requires that there is no heat flux across the axis, nor flow, nor shear stress, so both Ψ and ω are zero there. Then for points on the axis, the discrete heat balance over the cylindrical control volumes (half-square cross section $h/2 \times h$) gives:

$$\frac{d}{dt}\frac{h^2}{24}\begin{pmatrix} \frac{1}{4} & \frac{5}{4} \\ \frac{25}{4} & \frac{11}{4} \\ \frac{6}{4} & \end{pmatrix} T + \frac{1}{2h}\begin{pmatrix} \begin{pmatrix} & 1 \end{pmatrix}\Psi & \begin{pmatrix} 1 & \end{pmatrix}\Psi \\ \begin{pmatrix} & 1 \end{pmatrix}\Psi & \begin{pmatrix} & -1 \\ & \end{pmatrix}\Psi \\ \begin{pmatrix} & -2 \end{pmatrix}\Psi & \end{pmatrix} T$$

$$-\frac{1}{Ma}\begin{pmatrix} & \frac{1}{2} & \\ & -3 & 2 \\ & \frac{1}{2} & \end{pmatrix} T \;=\; 0 \quad (73)$$

where the equation was scaled using the average $\bar{r} = h/4$. The homogeneous Dirichlet conditions on Ψ and ω apply to points on the axis, and for grid points neighboring the axis, the usual stencils apply; no special treatment is necessary.

The temperature at the grid point at the origin is determined by a small control volume (quarter-square cross section $h/2 \times h/2$) with specified surface heat flux and no flux (nor convection) through the axis:

$$\frac{d}{dt}\frac{h^2}{24}\begin{pmatrix} \frac{1}{4} & \frac{5}{4} \\ \frac{15}{4} & \frac{3}{4} \end{pmatrix} T \;+\; \frac{1}{2h}\begin{pmatrix} \begin{pmatrix} & 1 \\ & \end{pmatrix}\Psi & \\ & \begin{pmatrix} & -1 \\ & \end{pmatrix}\Psi \end{pmatrix} T$$

$$-\frac{1}{Ma}\begin{pmatrix} & \frac{1}{2} & \\ & -\frac{3}{2} & 1 \end{pmatrix} T = \frac{1}{Ma}\frac{4}{h}\int_0^{h/2} q(r) r\, dr \quad (74)$$

Again, at the origin, both Ψ and ω are zero (note the two boundary conditions on vorticity are consistent at this point, due to the symmetry). Hence, the usual surface flow equations apply to the grid point next to the origin.

At the far boundaries of the computational domain, the boundary condition on the heat diffusion equation in the solid is that it decays in the same way as the spherically symmetric solution for a point source:

$$\nabla T = \frac{\partial T}{\partial R}\hat{\mathbf{R}} = -\frac{T}{R}\hat{\mathbf{R}} = -T\frac{r}{R^2}\hat{\mathbf{r}} - T\frac{z}{R^2}\hat{\mathbf{z}} \quad (75)$$

where $R \equiv \sqrt{r^2 + z^2}$. This allow the heat flux across the artificial boundary to be computed in terms of the temperature there, a Robin type boundary condition. Below we give the discrete equations for the two edges (half-square volumes) and three corners (quarter-square volumes) where this boundary condition is applied.

At the edge where r is at its maximum the stencil is given by

$$\frac{d}{dt}\frac{h^2}{24}\begin{pmatrix} & \frac{3}{2}-\frac{3}{8}\epsilon & \\ 2-\frac{11}{16}\epsilon & 7-\frac{25}{16}\epsilon & \\ 1-\frac{5}{16}\epsilon & \frac{1}{2}-\frac{1}{16}\epsilon & \end{pmatrix} T - \frac{1}{Ma}\begin{pmatrix} & \frac{1}{2}-\frac{1}{8}\epsilon-\frac{1}{8}\rho & \\ 1-\frac{1}{2}\epsilon & -2+\frac{3}{4}\epsilon-\frac{3}{4}\rho & \\ & \frac{1}{2}-\frac{1}{8}\epsilon-\frac{1}{8}\rho & \end{pmatrix} T = 0$$

where $\rho \equiv hr/(r^2+z^2)$.

At the edge where z is at its maximum the stencil is

$$\frac{d}{dt}\frac{h^2}{24}\begin{pmatrix} \frac{1}{2}-\frac{3}{16}\epsilon & 7-\frac{5}{16}\epsilon & \frac{3}{2}+\frac{1}{2}\epsilon) \\ 1-\frac{5}{16}\epsilon & 2+\frac{5}{16}\epsilon & \end{pmatrix} T - \frac{1}{Ma}\begin{pmatrix} \alpha & \beta & \gamma \\ & 1 & \end{pmatrix} T = 0$$

where

$$\alpha \equiv \frac{1}{2} - \frac{1}{4}\epsilon - \frac{1}{8}(1 - \frac{1}{3}\epsilon)\zeta, \quad \beta \equiv -2 - \frac{3}{4}\zeta, \quad \gamma \equiv \frac{1}{2} + \frac{1}{4}\epsilon - \frac{1}{8}(1 + \frac{1}{3}\epsilon)\zeta,$$

and $\zeta \equiv hz/(r^2 + z^2)$.

At the corner where both r and z are at a maximum the stencil is

$$\frac{d}{dt}\frac{h^2}{24}\begin{pmatrix} \frac{1}{2} - \frac{3}{16}\epsilon & 4 - \frac{15}{16}\epsilon \\ 1 - \frac{5}{16}\epsilon & \frac{1}{2} - \frac{1}{16}\epsilon \end{pmatrix} T - \frac{1}{Ma}\begin{pmatrix} \mu & \nu \\ & \xi \end{pmatrix} T = 0$$

where

$$\mu \equiv \frac{1}{2} - \frac{1}{4}\epsilon - \frac{1}{8}(1 - \frac{1}{3}\epsilon), \quad \nu \equiv -1 + \frac{3}{8}\epsilon - \frac{3}{8}[\rho + (1 - \frac{2}{9}\epsilon)\zeta],$$

and

$$\xi \equiv \frac{1}{2} - \frac{1}{8}\epsilon - \frac{1}{8}\rho.$$

At the corner where $r = 0$ and z is at a maximum we have the stencil

$$\frac{d}{dt}\frac{h^2}{24}\begin{pmatrix} \frac{5}{2} & 2 \\ \frac{3}{2} & \end{pmatrix} T - \frac{1}{Ma}\begin{pmatrix} -\frac{3}{2} - \frac{1}{3}\zeta & 1 - \frac{1}{6}\zeta \\ \frac{1}{2} & \end{pmatrix} T = 0.$$

Finally, at the corner where r is maximum and $z = 0$ the stencil is

$$\frac{d}{dt}\frac{h^2}{24}\begin{pmatrix} & \frac{3}{2} - \frac{3}{8}\epsilon \\ \frac{3}{2} - \frac{1}{2}\epsilon & 3 - \frac{5}{8}\epsilon \end{pmatrix} T - \frac{1}{Ma}\begin{pmatrix} & \frac{1}{2} - \frac{1}{8}\epsilon - \frac{1}{8}\rho \\ \frac{1}{2} - \frac{1}{4}\epsilon & -1 + \frac{3}{8}\epsilon - \frac{3}{8}\rho \end{pmatrix} T = 0.$$

Tracking the Phase-Change Interface

One of the biggest challenges in models of phase change is the tracking over time of the position of the two-phase interface. As one of the main goals of the current research is the examination of the effects of thermocapillary convection on the interface shape, great care is necessary in accurately modeling the geometry and dynamics of the phase change process.

The grid structure must be modified near the interface. (While it would be possible to quantize the interface position to lie on grid points, that would make moving the interface difficult and would introduce errors that would be magnified in the multilevel representation.) We represent the interface as piecewise linear between the points at which it crosses the diagonals of the main grid, which have slopes equal to 1. This representation assumes that the interface orientation never reaches an angle of 135° (or −45°) relative to the surface (i.e., parallel to the main diagonals); this seems reasonable, considering the interface is an isotherm that meets the surface at 90° and

must end at 0° at the axis. (A more general approach would include representations for several different local grid orientations.)

The movement of the interface through melting or solidification is governed by the local heat balance near the interface. Hence the main requirement for the control volume around each interface point (along the diagonals) is that the volume contain the interface both at the current time and at the next time step, that is, the control volumes must allow room for movement. (Then for the next time step, new control volumes may be used.) Hence, not only the current interface position, but also an estimate of the future position, is required to construct the current local grid. An alternate approach is to adjust the solidification timescale parameter λ at each time step to constrain the maximum motion of the interface to remain within the interface control volumes; physically this would correspond to time-dependent latent heat L.

To keep the geometry as simple as possible while allowing the interface points to move along the main diagonals, we construct the control volumes on a diagonal grid. (Here we refer to the control volumes by their cross sections in the (r, z) plane.) The main diagonals are spaced a distance $h/\sqrt{2}$ apart, and control volume boundaries in that direction lie midway between them. Control volume boundaries in the perpendicular direction are spaced the same, unless such boundary would cross the current or predicted interface, in which case that segment is removed, giving a double-wide volume $(\sqrt{2}h \times h/\sqrt{2})$. [Note: it is conceivable that, if the interface orientation exceeds 90°, triple-wide control volumes may be necessary.] Then any grid points within the interface control volumes are removed. If space remains between the interface control volume and the remaining regular grid, an auxiliary grid point is inserted on the diagonal a distance $h/\sqrt{2}$ from the regular grid point, with its diagonal square control volume $(h/\sqrt{2} \times h/\sqrt{2})$. [Note: to simplify the programming, the auxiliary points could be omitted; then the control volumes for the interface points will be either single width (no grid point removed) or triple width (one grid point removed).] Then the control volumes for the regular grid points adjoining this diagonal grid are pentagons in one of three configurations: at an "inside" corner with one diagonal side, two regular sides, and two regular half-sides; at a straight edge, either horizontal or vertical, with one regular side, two regular half-sides, and two diagonal sides; or, at an "outside" corner with three diagonal sides and two regular half-sides.

The auxiliary grid points form triangular elements with neighboring regular grid points and/or neighboring auxiliary grid points. This leaves trapezoidal elements adjoining the interface. Note that triangulating these trapezoids could result in very complicated relations between elements and volumes. Therefore we use a "warped" bilinear interpolation on these trapezoidal elements.

Where the interface intersects the surface or the axis, the grid must be further modified to track these important points. This involves computing the heat balance on a diagonal surface (or axis) control volume and tracking the position of the interface along the diagonal. Depending on the proximity of the interface point on the diagonal to the surface (or axis), then either the interface is extrapolated from the point inside the surface perpendicularly to the surface or the "interface point" on the diagonal

outside the surface is used to linearly interpolate the interface to the surface.

The interface is defined as the isotherm where $T = 1$, and on the interface the fluid velocity is zero (no slip), and so $\Psi = 0$. The unknown vorticity at interface points is determined by the stream function equation integrated over the liquid portion of the control volume; here the circulation can be calculated (with no contribution along the interface, due to no slip) to find the unknown strength of the vorticity tube:

$$\iint_{A_l} \omega \, dr \, dz = \oint_{C_l} \hat{\mathbf{t}} \cdot \mathbf{u} \, dl \tag{76}$$

where A_l is the liquid area, with bounding curve C_l. (Note that this equation contains no time derivative.)

The only remaining unknown is the future position (along the diagonal) of the interface point. This is governed by the heat balance over the liquid and solid portions of the control volume:

$$\begin{aligned} \lambda \, Ma^{-1} \frac{d}{dt} \iint_{A_l} r \, dr \, dz \;\; = \;\; & \\ & -\frac{d}{dt} \iint_{A_l + A_s} T \, r \, dr \, dz \\ & - \oint_{C_l} \hat{\mathbf{n}} \cdot (\mathbf{u} T) \; r \, dl \\ & + Ma^{-1} \oint_{C_l + C_s} \hat{\mathbf{n}} \cdot \nabla T \, r \, dl \end{aligned} \tag{77}$$

where $A_l + A_s$ indicates the entire control volume, with bounding curve $C_l + C_s$. (Note that A_l and C_l vary over the time step, while the control volume as a whole does not.) The interpretation is that the heat coming in by convection and diffusion goes to raise the temperature inside (though the interface temperature is fixed) and to melt some solid, increasing the liquid portion of the volume (the first term).

The discrete equations are very complicated for regular grid points bordering the diagonal interface grid and for interface points, and so are not reproduced here. To guard against typographical errors, the stencils were derived using the symbolic mathematics capabilities of the *Maple* software ([6]). *Maple* converted the resulting expressions into C language code, which were cut and pasted directly into our simulation code.

The diagonal grid around the interface requires local diagonal coordinates. We call these (x, y), where

$$\begin{array}{ll} x = z + r & \\ y = z - r & \text{so that} \end{array} \qquad \begin{array}{l} r = (x - y)/2 \\ z = (x + y)/2 \end{array} \tag{78}$$

Then the velocity becomes

$$\mathbf{u} = -\frac{\sqrt{2}}{r} \frac{\partial \Psi}{\partial y} \hat{\mathbf{x}} + \frac{\sqrt{2}}{r} \frac{\partial \Psi}{\partial x} \hat{\mathbf{y}} \tag{79}$$

Note that the (x, y) coordinates are scaled down in length by a factor of $\sqrt{2}$ relative to the (r, z) coordinates, and on the diagonal grid the values of the (x, y) coordinates are integer multiples of h (rescaled). In the area integrals, the Jacobian gives $dr\,dz = dx\,dy/2$, but in each of the line integrals, the scaling of the differential is exactly compensated by the scaling of the derivative (with respect to x or y). The slight complication of rescaling is more than offset by the simplification of the algebra; otherwise factors of $\sqrt{2}$ would abound. The bilinear interpolation for the trapezoidal elements is also in terms of the (x, y) coordinates, both to simplify integration with respect to the diagonal coordinates, and to avoid the singular case where the trapezoid is a diagonal perfect square, which cannot be interpolated with a bilinear form in (r, z).

Conclusion

In this preliminary work we have developed a finite volume element method for determining the shape of the weldpool. The governing equations and boundary conditions have been discretized in space, and a time-stepping method can be applied to solve the equations. An FAC method has been devised for resolving the fine details near the moving interface and is being implemented as part of the continuing research.

The basic numerical methods discussed have been implemented in code and tested. A future report will describe the details of the time-stepping, the FAC resolution near the interface, and the numerical results on the total problem.

Acknowledgements

This work was supported by the Office of Naval Research, Materials Division (contract N0001492WR24009).

REFERENCES

[1] Milton Abramowitz and Irene A. Stegun. *Handbook of Mathematical Functions.* Dover Publications, Inc., New York, 1965.

[2] D. Canright. Thermocapillary flow near a cold wall. *Phys. Fluids*, 6:1415–1424, 1994.

[3] C. L. Chan, M. M. Chen, and J. Mazumder. Asymptotic solution for thermocapillary flow at high and low Prandtl numbers due to concentrated surface heating. *J. Heat Transfer*, 110:140–146, 1988.

[4] M. M. Chen. Thermocapillary convection in materials processing. In S. K. Samanta, R. Komandiri, R. McMeeking, M. M. Chen, and A. Tseng, editors, *Interdisciplinary Issues in Materials Processing and Manufacturing*, pages 541–557, ASME, 1987.

[5] Stephen F. McCormick. *Multilevel Adaptive Methods for Partial Differential Equations.* Society for Industrial and Applied Mathematics, Philadelphia, 1989.

[6] Waterloo Maple Software. *Maple V, Release 3.* Waterloo, Ontario, Canada, 1994. (X-windows version for Unix workstations).